Electr Eng (2008) 90:199–207
DOI 10.1007/s00202-007-0074-2

ORIGINAL PAPER

Single-input fuzzy-like moving sliding surface approach to the sliding mode control

Ferhun Yorgancıoğlu · Hasan Kömürcügil

Received: 9 February 2007 / Accepted: 5 May 2007 / Published online: 14 June 2007

Abstract A new approach to the sliding mode control of second-order nonlinear systems is introduced in continuous-time. A single-input fuzzy logic controller is used to continuously compute the slope of the sliding surface, with the result that the sliding surface is rotated in such a direction that tracking performance of the system under control is improved. The proposed fuzzy moving sliding surface approach with a one-dimensional rule base (FMSS-1D) reduces huge number of linguistic fuzzy rules significantly. However, it is shown that the input/output relation of the single-input fuzzy rule base is very close to the input/output relation of a straight line. Therefore, a single-input fuzzy-like moving sliding surface (FLMSS) approach using an approximate line function is then proposed. It is shown that the proposed control approaches have better tracking performance than the conventional sliding mode control with fixed sliding surface. The proposed moving sliding surface approaches are applied to balance an inverted pendulum on a cart. Computer simulations are presented to show the effectiveness of the proposed methods and to make a quantitative comparison with the classical sliding-mode controller with fixed sliding surface method existing in literature.

Keywords Second order nonlinear system · Sliding mode control · Fuzzy logic control

F. Yorgancıoğlu (✉) · H. Kömürcügil
Computer Engineering Department,
Eastern Mediterranean University, North Cyprus,
via Mersin 10, Gazimağusa, Turkey
e-mail: ferhun.yorgancioglu@emu.edu.tr

H. Kömürcügil
e-mail: hasan.komurcugil@emu.edu.trr

1 Introduction

In recent years, the sliding mode control (SMC) theory has become very popular and therefore, it has been studied widely for the control of nonlinear systems [1–3]. The reason behind this popularity is the attractive advantages of SMC. The main advantage of SMC is that once the system states reach the sliding surface, the system remains on this surface and the states go to origin while the system is insensitive to parameter variations. In addition to this advantage, the SMC method offers a simple algorithm that can be implemented easily. Besides this advantage, the SMC using a conventional time-invariant (fixed) sliding surface has the fundamental disadvantage that when the system states are in the reaching mode, the tracking error cannot be controlled directly and hence, the system becomes sensitive to parameter variations. This sensitivity can be minimized or eliminated if the reaching mode duration is shortened. Moreover, finding the optimum value of the slope requires tedious work and usually, it is a complicated task [4]. Thus, how to adjust (or change) the slope of a sliding surface is an important topic in the sliding mode controlled nonlinear systems. Several methods [5–11] exist in literature aiming at to eliminate the sensitivity during the reaching mode. In [5], to eliminate reaching phase, the condition of having zero initial errors is assumed. However, initial errors may be located arbitrarily in the error state–space. The methods proposed in [6,7] are based on rotating or shifting the sliding surface to guarantee the existence of the sliding mode from the initial point of motion. In [8–11], completely different approaches based on qualitative control rules, namely, fuzzy logic control (FLC) are proposed to cope with the parameter sensitivity during the reaching mode. However, the common disadvantage of the methods presented in [10,11] is that they are based on two-dimensional (2D) fuzzy rule base which increases the computation time of the control input significantly.

In this paper, a single-input fuzzy moving sliding surface approach to the sliding mode control of second-order nonlinear systems is presented. The main advantage of the proposed control method is that the slope of the sliding surface is not fixed, but it is changed continuously according to the values of the error variables. Each time the slope is modified, the sliding surface (or sliding line) rotates in clockwise or counterclockwise direction so as to achieve the desired performance. The change in slope is computed by fuzzy logic rules using one dimensional (1D) rule base. Using 1D rule base reduces the number of rules needed to compute the slope and the computation time significantly [12]. Furthermore, it is shown that the single-input fuzzy moving sliding surface approach can be approximated by a line equation. Finally, the computer simulation results are given to verify the effectiveness of the proposed control methods.

2 Conventional sliding mode control

Consider the following single-input, second-order nonlinear system

$$\dot{x}_1(t) = x_2(t) \tag{1}$$

$$\dot{x}_2(t) = f(\mathbf{x}) + b(\mathbf{x})u(t) \tag{2}$$

where $\mathbf{x} = [x_1, x_2]^{\mathrm{T}}$ is the state vector, $f(\mathbf{x})$ and $b(\mathbf{x})$ are nonlinear functions representing system dynamics, and $u(t)$ is the control input. The control objective is to design a control input $u(t)$ to force the system states to track a desired input signal $x_d(t)$. Let $e(t)$ be the tracking error between the actual and the desired trajectory as follows

$$e(t) = x_1(t) - x_{1d}(t) \tag{3}$$

Taking the time derivative of both sides of (3) gives

$$\dot{e}(t) = x_2(t) - x_{2d}(t) \tag{4}$$

where $x_{1d}(t)$ and $x_{2d}(t) = \dot{x}_{1d}(t)$ are the desired trajectories for the states $x_1(t)$ and $x_2(t)$, respectively. The sliding function $S(t)$ is defined as a linear combination of the error variables [5] as

$$S(t) = \lambda e(t) + \dot{e}(t), \quad \lambda > 0 \tag{5}$$

where λ is a positive constant that determines the slope of the sliding surface. The sliding mode ($S(t) = 0$) is described by the first order equation

$$\dot{e}(t) = -\lambda e(t) \tag{6}$$

with solution

$$e(t) = e(0)\exp(-\lambda t) \tag{7}$$

It is obvious from (7) that the system dynamics depend on λ. For instance, a high value of λ is expected to move the error variables on the sliding surface faster. On the other hand, if the value of λ is chosen too high, it can cause an overshoot in the system states and an instability.

In general, the motion of an SMC system can be divided into two modes: the reaching mode and the sliding mode. During the reaching mode, the error variables are driven to the sliding surface by implementing a suitable reaching control strategy. On the other hand, when the error variables are on the sliding surface, the system is said to be in the sliding mode in which the errors are driven to the origin ($e(t) = \dot{e}(t) = 0$) by implementing an equivalent control strategy.

Now, taking the time derivative of the sliding function $S(t)$ gives

$$\dot{S}(t) = \lambda \dot{e}(t) + \ddot{e}(t) \tag{8}$$

By substituting (4) into (8) and making use of (1) and (2), we can obtain

$$\begin{aligned} \dot{S}(t) &= \lambda \dot{e}(t) + \dot{x}_2(t) - \dot{x}_{2d}(t) \\ &= \lambda \dot{e}(t) + f(\mathbf{x}) + b(\mathbf{x})u(t) - \ddot{x}_{1d}(t) \end{aligned} \tag{9}$$

When the system is in the sliding mode along (8), we have $S(t) = \dot{S}(t) = 0$. Equating (9) to zero and solving for $u(t)$ gives the following equivalent control expression

$$u_{\mathrm{eq}}(t) = \frac{1}{b(\mathbf{x})}[\ddot{x}_{1d}(t) - f(\mathbf{x}) - \lambda \dot{e}(t)], \quad b(\mathbf{x}) \neq 0 \tag{10}$$

When the equivalent control is applied to the system, the error variables are forced to move towards the origin immediately. As a result, the desired dynamic behavior can be achieved after the sliding mode starts. However, the equivalent control may not be able to move the error variables from reaching mode to sliding mode. Therefore, an additional control action (reaching control) is needed that should be applied to the system together with the equivalent control [5] as

$$u(t) = u_{\mathrm{eq}}(t) - K\,\mathrm{sgn}\,[S(t)] \tag{11}$$

where $K > 0$ is a positive real number to be selected and sgn[.] is the signum function. For stability, the existence condition $S(t)\dot{S}(t) < 0$ for the reaching mode must be satisfied. Hence, the total control input becomes

$$u(t) = \frac{1}{b(\mathbf{x})}[\ddot{x}_{1d}(t) - f(\mathbf{x}) - \lambda \dot{e}(t)] - K\,\mathrm{sgn}\,[S(t)] \tag{12}$$

It is well known that the controller shown in (12) suffers from high frequency switching near the sliding surface and chattering occurs due to signum function [2,5]. In order to avoid chattering, a boundary layer is introduced with width ϕ. Hence, signum function can be easily replaced by a saturation function sat$\left[\frac{S(t)}{\phi}\right]$ that is defined as

$$\mathrm{sat}(z) = \begin{cases} \mathrm{sgn}(z), & \text{if } |z| \geqslant 1 \\ z, & \text{if } |z| < 1 \end{cases} \tag{13}$$

The conventional SMC with the predetermined fixed slope (λ) degrades the desired dynamic behavior of the system after the beginning of motion. Robust tracking can be guaranteed during the sliding mode. However, since the tracking error cannot be controlled directly, the robustness cannot be guaranteed in the reaching mode [7]. The robustness of system can be improved if the duration of the reaching mode is shortened. Therefore, it is most desirable if a control strategy (which would shorten the reaching time and achieve fast tracking of the system state variables and preserve the robustness property) based on a moving sliding surface could be developed for the nonlinear systems.

3 Fuzzy moving sliding surface approach

In this section, we combine the attractive features of SMC and FLC to introduce a sliding mode control strategy based on fuzzy moving sliding surface. Now, consider the sliding surface depicted in Fig. 1. It is clear that the controller with $\lambda_{\min}$ leads to slower error convergence and longer tracking time. On the other hand, the controller with $\lambda_{\max}$ leads to faster error convergence, but the tracking accuracy can be degraded. Therefore, it is obvious that there is a trade-off between error convergence time and tracking time. The rotation (or movement) of the sliding surface can be achieved if the value of λ is updated according to the values of the error variables $e(t)$ and $\dot{e}(t)$ [10]. Note that for the sake of stability, the positiveness of λ must be preserved during this rotation process. From now on, the slope of the sliding surface computed by fuzzy logic rules will be represented by λ_{2D}^F for 2D rule base and by λ_{1D}^F for 1D rule base.

The dynamic behavior of the FLC is characterized by a set of linguistic rules based on expert knowledge. These linguistic (fuzzy) rules are of the form [10]:

$$\text{IF } e(t) \text{ is } E(t) \text{ and } \dot{e}(t) \text{ is } \dot{E}(t) \text{ THEN } \lambda_{2D}^F \text{ is LAMDA}_{2D} \tag{14}$$

where $E(t)$, $\dot{E}(t)$, and LAMDA$_{2D}$ are the fuzzy sets of $e(t)$, $\dot{e}(t)$, and λ_{2D}^F, respectively. It should be pointed out here that, we assume both $e(t)$ and $\dot{e}(t)$ are scaled down to the unit range of $[-1, +1]$ before applying them as fuzzy inputs to the FLC (process of fuzzification). Furthermore, it is obvious that the inputs ($e(t)$ and $\dot{e}(t)$) to FLC can have negative and positive values. However, the output of the FLC must be always positive due to the positive slope requirement ($\lambda_{2D}^F > 0$). For this reason, the rule base of the FLC plays a very important role here and should be constructed in such a way that the performance of the system is improved. The membership functions for the inputs are represented by negative big (NB), negative medium (NM), negative small (NS), zero (ZE), positive small (PS), positive medium (PM), and positive big (PB), respectively. Similarly, the membership functions for the slope λ_{2D}^F are represented by very very small (VVS), very small (VS), small (S), medium (M), big (B), very big (VB), and very very big (VVB), respectively. When every seven membership functions (see Fig. 2) for $e(t)$, $\dot{e}(t)$, and λ_{2D}^F are used, the 2D rule base shown in Table 1 with 49 fuzzy rules [10] can be constructed. The input/output relation of these fuzzy rules is shown in Fig. 3. This 2D rule base has two interesting properties. Firstly, it can be seen from Fig. 1 and Table 1 that when the representative point (RP) falls into the second and fourth quadrants, the rules are arranged in such a manner that the sliding surface moves in the same direction as the system. That is, the sliding surface rotates in clockwise direction. Secondly, when the RP falls into first and third

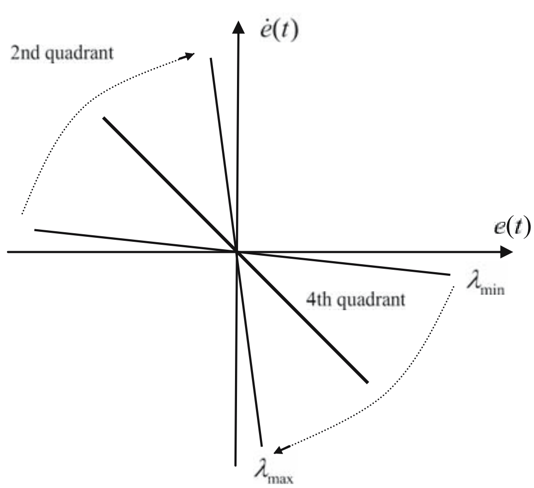

Fig. 1 Sliding surface with maximum, medium, and minimum slope values

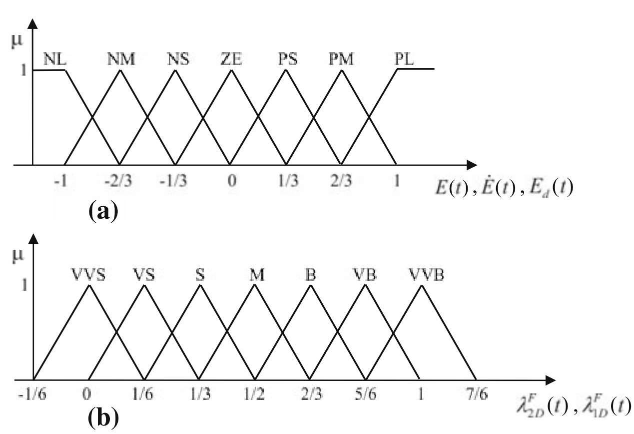

Fig. 2 (a) Fuzzy input membership functions (b) Fuzzy output membership functions

Table 1 Two-dimensional rule base used to compute λ_{2D}^F(t)

$\lambda_{2D}^F(t)$	Error ($E(t)$)						
	NB	NM	NS	ZE	PS	PM	PB
Change-in-error ($\dot{E}(t)$)							
PB	M	B	VB	VVB	VB	B	M
PM	S	M	B	VB	B	M	S
PS	VS	S	M	B	M	S	VS
ZE	VVS	VS	S	M	S	VS	VVS
NS	VS	S	M	B	M	S	VS
NM	S	M	B	VB	B	M	S
NB	M	B	VB	VVB	VB	B	M

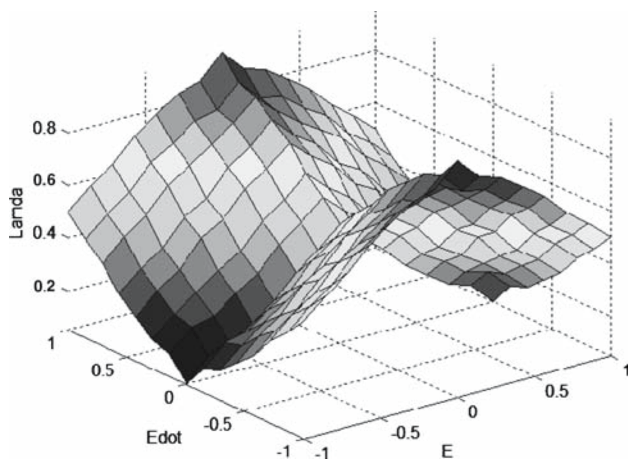

Fig. 3 The input/output relation of the fuzzy controller with 2D rule base

quadrants, the rules are defined in such a manner that the sliding surface rotates in counterclockwise direction in contrast to the ideas developed in [9], where shifting is applied for first and third quadrants. Hence, with this type of rule base we do not need to shift the sliding surface up or down to make the RP fall into second and fourth quadrants so as to apply the rotation strategy to shorten the time required to reach the sliding surface. However, the main disadvantage of the FLC with 2D rule base is that it requires $k \times n$ rules, where k is the number of linguistic values used for $e(t)$ and n is the number of linguistic values used for $\dot{e}(t)$. This means that with seven linguistic values used for both input variables of $e(t)$ and $\dot{e}(t)$, 49 rules will be needed to implement the proposed control scheme. However, a rule base constructed with 49 rules increases the computation time required compared to the case when a 1D rule base is utilized, which is the usual situation with most of the FLCs constructed for the SMCs so far. In the following section, the idea behind constructing a 1D rule base is studied extensively.

4 Single-input fuzzy and fuzzy-like moving sliding surface approaches

Now, let us reconsider the 2D rule base shown in Table 1. After a careful observation, one can easily see that the rules in each quadrant are mirror images of the rules in the adjacent quadrants. This interesting property can be explained as follows. When the system is in the first quadrant with $E(t) = \text{PM}$ and $\dot{E}(t) = \text{PM}$, the output of the FLC will be $\lambda_{2D}^F = M$. The same value for λ_{2D}^F can be obtained when at least one input signal changes its sign in adjacent quadrant as follows

$$\begin{aligned}
&\text{When } E(t) = \text{NM} \text{ and } \dot{E}(t) = \text{PM}\\
&\quad \Rightarrow \text{ The FLC output } \lambda_{2D}^F = M \text{(2nd quadrant)}\\
&\text{When } E(t) = \text{NM} \text{ and } \dot{E}(t) = \text{NM}\\
&\quad \Rightarrow \text{ The FLC output } \lambda_{2D}^F = M \text{(3rd quadrant)}\\
&\text{When } E(t) = \text{PM} \text{ and } \dot{E}(t) = \text{NM}\\
&\quad \Rightarrow \text{ The FLC output } \lambda_{2D}^F = M \text{(4th quadrant)}
\end{aligned}$$

Similarly, when the system is in the second quadrant with $E(t) = \text{NM}$ and $\dot{E}(t) = \text{PB}$, the output of the FLC will be $\lambda_{2D}^F = B$. The same value for λ_{2D}^F can be obtained when at least one input signal changes its sign in adjacent quadrant as follows

$$\begin{aligned}
&\text{When } E(t) = \text{PM} \text{ and } \dot{E}(t) = \text{PB}\\
&\quad \Rightarrow \text{ The FLC output } \lambda_{2D}^F = B \text{(1st quadrant)}\\
&\text{When } E(t) = \text{NM} \text{ and } \dot{E}(t) = \text{NB}\\
&\quad \Rightarrow \text{ The FLC output } \lambda_{2D}^F = B \text{(3rd quadrant)}\\
&\text{When } E(t) = \text{PM} \text{ and } \dot{E}(t) = \text{NB}\\
&\quad \Rightarrow \text{ The FLC output } \lambda_{2D}^F = B \text{(4th quadrant)}
\end{aligned}$$

Motivated with this important property, it seems that the number of the rules in the 2D rule base can be reduced considerably. The rule base reduction can be achieved by two scenarios. Firstly, we can use only rules of the first quadrant (only 16) to represent all cases (when $e(t)$ and $\dot{e}(t)$ falls into first, second, third, and fourth quadrants). This can be obtained simply by multiplying error variables with their signs (or calculating their absolute values). After multiplying them with their signs (and the process of fuzzification), they can be used as two fuzzy input variables to a 2D rule base having rules of the first region (or quadrant) of the phase plane. With this process, a significant reduction can be obtained in the rule base. With seven membership functions used for both input variables, we reduce rule base from 49 linguistic fuzzy rules to 16. Secondly, remembering the case in [12] of reducing rule bases of linear type, we can think about reducing it more to form only 1D case (to represent 2D rule base with only 7 rules). Obviously, using the same idea of reducing 49 rules to 16, we can easily proceed and use the same strategy but this time with calculating absolute magnitude differences between fuzzy inputs of the $e(t)$ and $\dot{e}(t)$ to form a single-input to be applied to a 1D rule base. The idea of formulating the new fuzzy input to the 1D rule base can be written as

$$E_d(t) = |E(t)| - \left|\dot{E}(t)\right| \tag{15}$$

where $E_d(t)$ is the magnitude difference in error variables. Hence, we form a single-input fuzzy variable $E_d(t)$ and correspondingly a 1D rule base having only 7 linguistic fuzzy rules of the following form

$$\text{IF } E_d(t) \text{ is ED THEN } \lambda_{1D}^F \text{ is LAMDA}_{1D} \tag{16}$$

where ED and LAMDA$_{1D}$ are the fuzzy sets of $E_d(t)$ and λ_{1D}^F shown in Fig. 2. Studying all cases available in the 2D rule base one can easily form a 1D rule base as shown in Table 2. The input/output relation of the fuzzy rules in 1D rule base is shown in Fig. 4. The corresponding block diagram of single-input fuzzy moving sliding surface based on SMC is depicted in Fig. 5. Obviously, the calculation of the time-varying slope of the SMC is less complicated compared to a case of having 2D rule base with 49 rules.

Table 2 One-dimensional rule base used to compute $\lambda_{1D}^F(t)$

$E_d(t)$	NB	NM	NS	ZE	PS	PM	PB
$\lambda_{ID}^F(t)$	VVB	VB	B	M	S	VS	VVS

In order to investigate the error involved in this rule base reduction, the mean squared error (MSE) defined in (17) between the surface plots of the two rule bases (2D and 1D) has been calculated.

$$\text{MSE} = \frac{1}{r} \sum_{E(t), \dot{E}(t), E_d(t) = -1}^{+1} (\hat{\varphi} - \varphi)^2 \tag{17}$$

where r represents the step size, φ represents a fuzzy value on the 2D surface, and $\hat{\varphi}$ represents the estimate of φ (a fuzzy value on the 1D surface). Fuzzy input variables $E(t)$, $\dot{E}(t)$, and $E_d(t)$ are obtained by scaling down the error variables $e(t)$ and $\dot{e}(t)$ into the unit range of $[-1, +1]$. This is known as fuzzification process. When the values of these fuzzified error variables are chosen to vary at discrete points apart from each other by a step size of 0.05 in the unit range that they are defined over the surface plots shown in Figs. 3 and 4, the MSE is calculated as 0.0012 unit^2. This calculation verifies that the 1D rule base can represent the 2D one.

The input/output relation shown in Fig. 4 looks like very close to a straight line. One can easily see that this input/output relation can be approximated by the following linear equation

$$\lambda^{\text{FL}}(t) = -0.45 E_d(t) + 0.5 \tag{18}$$

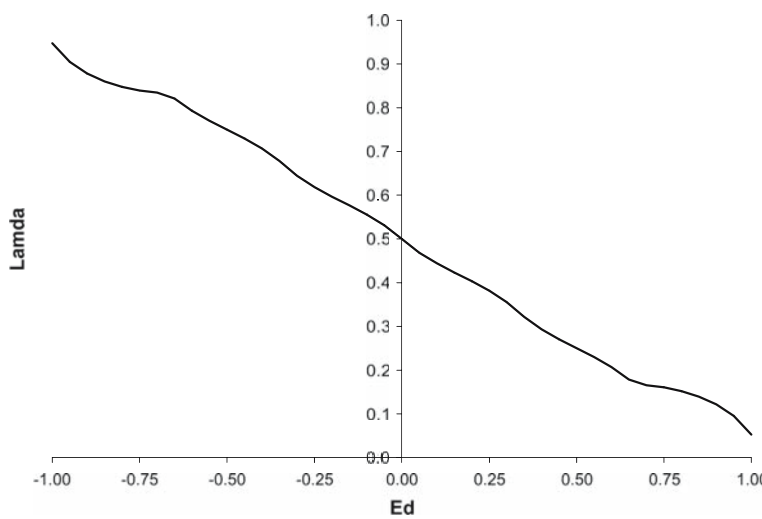

Fig. 4 The input/output relation of the fuzzy controller with 1D rule base

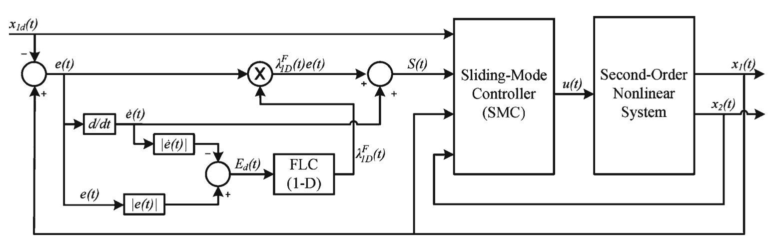

Fig. 5 Block diagram of the single input fuzzy moving sliding surface SMC using 1D rule base

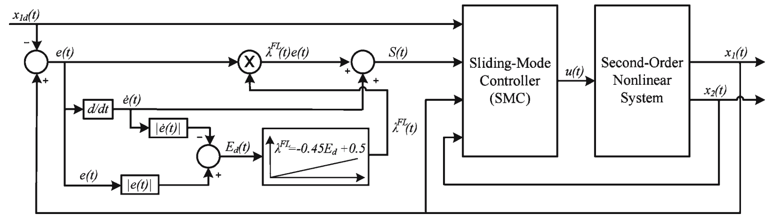

Fig. 6 Block diagram of the single-input fuzzy-like moving sliding surface SMC

where $E_d(t)$ is calculated as in (15) with -0.45 representing the slope of the straight line, 0.5 is intercept of the line, and λ^{FL} is the fuzzy-like calculated new slope. Here, we propose to replace the FLC block using 1D rule base shown in Fig. 5 by the approximated line equation given in (18). The corresponding block diagram of single-input fuzzy-like moving sliding surface based on SMC is depicted in Fig. 6.

5 Stability analysis

In this section, we show that the proposed control approaches have no stability problem. We start our stability analysis by considering the following Lyapunov function

$$V(t) = \frac{1}{2}S^2(t) \tag{19}$$

Taking time derivative of the Lyapunov function gives

$$\dot{V}(t) = S(t)\dot{S}(t) \tag{20}$$

It is well known from Lyapunov's stability Theorem that any linear or nonlinear system is globally asymptotically stable if $\dot{V}(t)$ is negative definite. Therefore, the existence condition $\left[\dot{V}(t) = S(t)\dot{S}(t)\right] < 0$ for the reaching mode must be satisfied. Substituting (5), (9), and (12) into (20) yields

$$\begin{aligned}\dot{V}(t) &= S(t)\{-b(\mathbf{x})K \operatorname{sgn}[S(t)]\}\\ &= -S(t)b(\mathbf{x})K \operatorname{sgn}[S(t)]\end{aligned} \tag{21}$$

Assuming that $b(\mathbf{x}) > 0$, it is clear from (21) that the derivative of Lyapunov function is always negative ($[\dot{V}(t) = S(t)\dot{S}(t)] < 0$) regardless of the sign of $S(t)$. This means that the system trajectory is driven and forced towards the sliding surface and remain sliding on it until the origin is reached asymptotically.

6 Computer simulations

In order to verify the theoretical considerations and test the performance of the proposed control approaches, the inverted pendulum system (or the cart-pole system) shown in Fig. 7

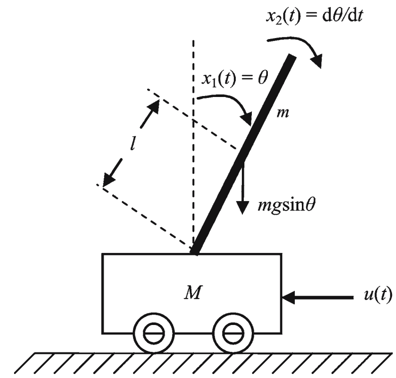

Fig. 7 The inverted pendulum on a cart

has been simulated using Matlab/Simulink. The closed-loop system is simulated with a time-step (step size) of 0.01 s using the Runge–Kutta method. The switching control gain is chosen as $K = 125$ for all simulation studies. Slope of the SMC with fixed sliding surface is selected as $\lambda = 5$. It is important to note here that in order to have $\lambda = \lambda^F_{2D} = \lambda^F_{1D} = \lambda^{\mathrm{FL}} = 5$ in the steady-state, the output scaling factor (output gain) of both fuzzy (using 2D or 1D rule bases) and fuzzy-like controllers is intentionally selected as 10. Since the output scaling factor affects the output value of FLC (slope), its value should be selected in such a way that all controllers will have a final slope value of 5 (for the sake of comparison purposes) in the steady-state. The dynamic behavior of the inverted pendulum system can be described by the following nonlinear equations [13]

$$\dot{x}_1(t) = x_2(t) \tag{22}$$

$$\dot{x}_2(t) = f(\mathbf{x}) + b(\mathbf{x})u(t) \tag{23}$$

where

$$f(\mathbf{x}) = \frac{g\sin(x_1) - mlax_2^2\sin(x_1)\cos(x_1)}{4l/3 - mla\cos^2(x_1)} \tag{24}$$

$$b(\mathbf{x}) = \frac{a\cos(x_1)}{4l/3 - mla\cos^2(x_1)}. \tag{25}$$

In above equations, $x_1(t)$ is the angular position of the pole from the vertical, $x_2(t)$ is the angular velocity (i.e. change in the angular position), m is the mass of the pole, M is the mass of the cart, a is $1/(m+M)$, l is the half length of the pole.

Table 3 Parameters of the inverted pendulum on a cart

m	Mass of the pole	0.05 kg
M	Mass of the cart	1 kg
l	Half length of the pole	0.5 m
g	Acceleration due to gravity	9.8 m/s^2

The system parameters selected for the simulation studies are given in Table 3.

As performance measure for a quantitative comparison, we use integral of absolute error (IAE) and integral of time absolute error (ITAE) that are defined as

$$\mathrm{IAE} = \int |e(t)|\mathrm{d}t \tag{26}$$

$$\mathrm{ITAE} = \int t|e(t)|\mathrm{d}t \tag{27}$$

Figure 8 shows the transient response of the system states, error convergence, phase portrait, and the slope values

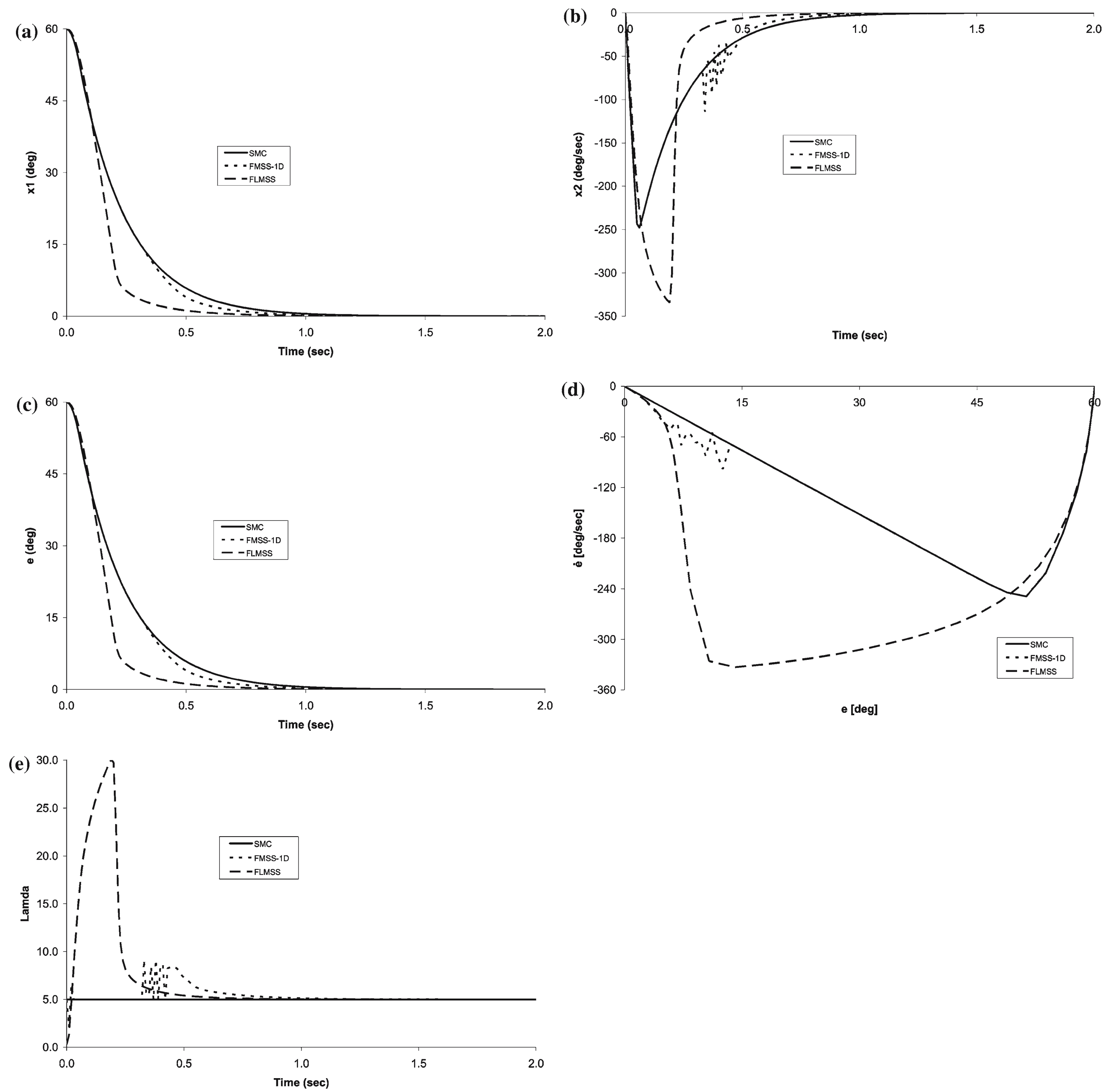

Fig. 8 Transient response of the inverted pendulum system when $x_{1d}(t) = 0$ for: (**a**) $x_1(t)$, (**b**) $x_2(t)$, (**c**) $e(t)$ (**d**) phase portrait of the error-state space, and (**e**) λ

obtained for SMC, FMSS-1D, and FLMSS methods when $x_{1d}(t) = 0$. The initial condition of the pole angle is assumed to be $x_1(0) = 60°$. It is clear from Figs. 8a and 8b that both FMSS-1D and FLMSS approaches are faster in transient response in terms of angular position and angular velocity of the pole. Error convergence and phase portrait shown in Figs. 8c and 8d are also faster in case of moving sliding surface cases. It is shown in Fig. 8e that a higher ($\lambda > 5$) dynamic slope is required to force the system to reach its steady-state earlier. This fast dynamic response of the system with moving sliding surface methods can be considered as an indication of the shortening the reaching mode time. The corresponding performance measures are given in Table 4 where moving sliding surface methods give better performance compared to the SMC with fixed sliding surface.

Figure 9 shows the transient response of the system state $x_1(t)$, error convergence, phase portrait, and the slope values obtained for SMC, FMSS-1D, and FLMSS methods when $x_{1d}(t) = \frac{\pi}{10}[\sin(t) + 0.3\sin(3t)]$. The initial condition of the pole angle is assumed to be $x_1(0) = 30°$. It is clear from Fig. 9a that both FMSS-1D and FLMSS approaches are faster in transient response in terms of angular position of the pole. Error convergence and phase portrait shown in Figs. 9b and 9c are also faster in case of moving sliding surface approaches (FMSS-1D and FLMSS). It is shown in Fig. 9d that a higher ($\lambda > 5$) dynamic slope is required to force the system to reach its steady-state earlier. This fast dynamic response of the system with moving sliding surface methods can be considered as an indication of the shortening the reaching mode time. The corresponding performance measures are given in Table 5 where moving sliding surface methods give better

Table 4 IAE/ITAE results calculated for the case when pole starts from an initial angle

	SMC using sgn	SMC using sat	FMSS-2D	FMSS-1D	FLMSS
IAE	17.09	13.82	13.37	13.11	9.30
ITAE	6.43	2.82	2.51	2.37	1.09

Table 5 IAE/ITAE results calculated for tracking control

	SMC using sgn	SMC using sat	FMSS-2D	FMSS-1D	FLMSS
IAE	21.61	6.38	5.93	5.72	3.16
ITAE	50.59	1.53	1.29	1.20	0.63

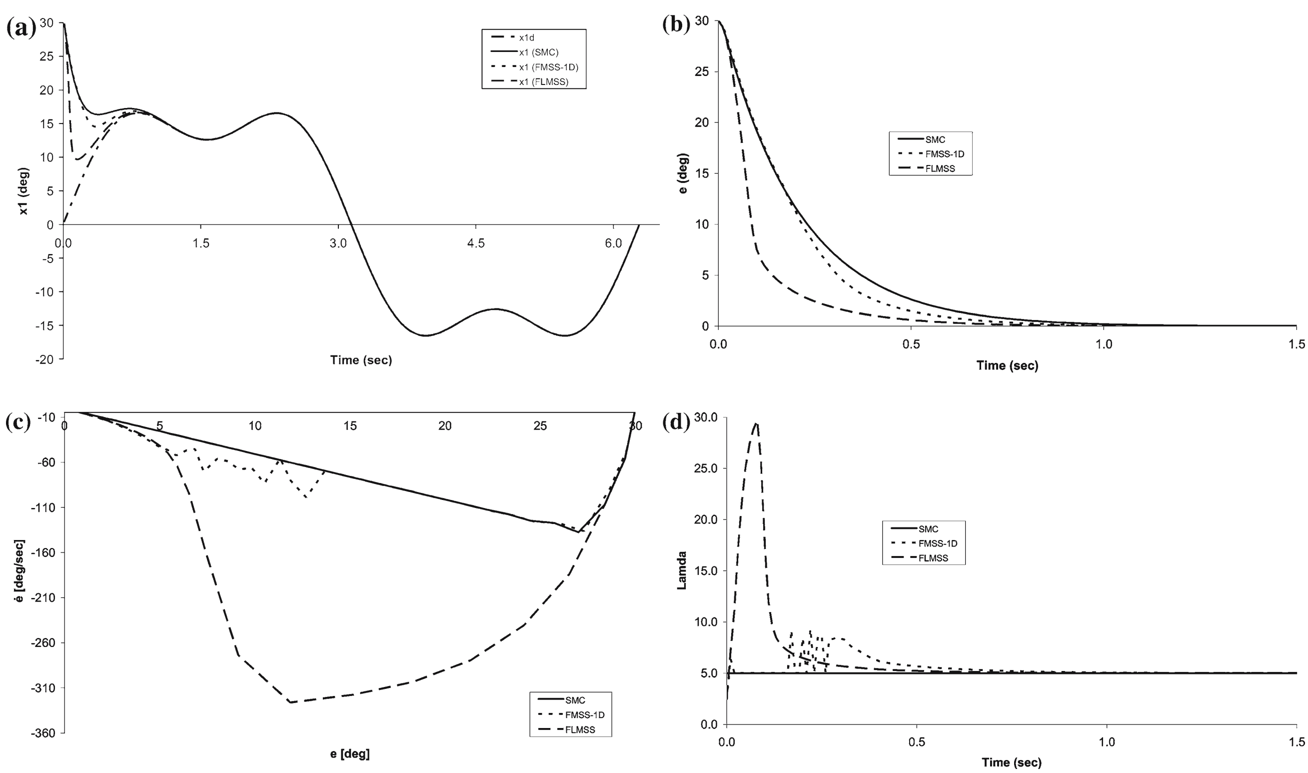

Fig. 9 Transient response of the inverted pendulum system when $x_{1d}(t) = \frac{\pi}{10}[\sin(t) + 0.3\sin(3t)]$ for: (**a**) $x_1(t)$ versus $x_{1d}(t)$, (**b**) $e(t)$, (**c**) Phase portrait of the error-state space, and (**d**) λ

performance compared to the SMC with fixed sliding surface.

7 Conclusions

In this study, a new approach to the sliding mode control of second-order nonlinear systems is introduced in continuous-time. A single-input fuzzy logic controller is used to continuously compute the slope of the sliding surface, with the result that the sliding surface is rotated in such a direction that tracking performance of the system under control is improved. It is shown that the proposed FMSS-1D reduces huge number of linguistic fuzzy rules significantly. In spite of its easy implementation, it can be simplified by an approximate line equation similar to its input/output relation. Therefore, the FLMSS approach using an approximate line function is then proposed. It is shown that the proposed control approaches have better tracking performance than the conventional sliding mode control with fixed sliding surface. The proposed moving sliding surface approaches are applied to balance an inverted pendulum on a cart. Computer simulations presented show that the proposed moving sliding surface approaches exhibit faster transient response in the system states leading to a faster error convergence and reaching time.

References

1. Utkin VI (1977) Variable structure systems with sliding modes. IEEE Trans Automat Control 22:212–222
2. Hung JC, Gao W (1993) Variable structure control: a survey. IEEE Trans Ind Electron 40(1):2–21
3. Young KD, Utkin V, Özgüner Ü (1999) A control engineer's guide to sliding mode control. IEEE Trans Control Syst Technol 7(3):328–342
4. Ackermann J, Utkin V (1998) Sliding mode control design based on Ackermann's formula. IEEE Trans Automat Control 43(2):234–237
5. Slotine JJE, Li W (1991) Applied nonlinear control. Prentice-Hall, Englewood Cliffs
6. Choi SB, Park DW, Jayasuriya S (1994) A time-varying sliding surface for fast and robust tracking control of second-order uncertain systems. Automatica 30(5):899–904
7. Bartoszewicz A (1996) Time-varying sliding modes for second order systems. IEE Control Theory Appl 143(5):455–462
8. Lee H, Kim E, Kang HJ, Park M (1998) Design of a sliding mode controller with fuzzy sliding surfaces. IEE Control Theor Appl 145(5):411–418
9. Ha QP, Rye DC, Durrant-Whyte HF (1999) Fuzzy moving sliding mode control with application to robotic manipulators. Automatica 35:607–616
10. Yağız N, Hacıoğlu Y (2005) Fuzzy sliding modes with moving surface for the robust control of a planar robot. J Vibration Control 11:903–922
11. Tokat S, Eksin İ, Güzelkaya M (2003) New approaches for on-line tuning of the linear sliding surface slope in sliding mode controllers. Turkish J Elect Engi 11(1):45–59
12. Choi BJ, Kwak SW, Kim BK (2000) Design and stability analysis of single-input fuzzy logic controller. IEEE Trans Syst, Man, Cybern- Part-B 30(2):303–309
13. Ogata K (1997) Modern control engineering. Prentice-Hall, Upper Saddle River